RESEARCH ARTICLE-CIVIL ENGINEERING

Study on the Stability of Rock Slope Under the Coupling of Stress Field, Seepage Field, Temperature Field and Chemical Field

Dengxing Qu[1,2] · Yi Luo[3] · Xinping Li[3] · Gang Wang[2,3] · Guang Zhang[1] · Kun Xu[2,3]

Abstract

The research on the stability of rock slopes under the multi-field coupling has important theoretical and practical significance for the analysis and prevention of freeze–thaw disasters of engineering in cold regions. In this paper, COMSOL Multiphysics numerical simulation software and numerical simulation methods are adopted. Based on the coupling theory of rock stress field, seepage field, temperature field, and chemical field, and field test data, the stability of rock slope under the multi-field coupling is studied under the research background of the highway slope of Jinghe to Yining County of G577 line. Based on the study of multi-field coupling theory, a numerical calculation model is established, the rationality of the numerical calculation model is verified, and the maximum frozen thickness of the slope is determined. On this basis, the change rules of the relevant parameters such as stress, temperature, deformation and damage of the highway slope in the engineering area are studied. The slope stability analysis is performed based on the YAI slope stability evaluation method. The stability of the slope is analyzed from the freezing, thawing and freeze–thaw process states of the shallow layer of the slope. It provides a theoretical basis for engineering construction in cold region.

Keywords Multi-field coupling · Freeze–thaw cycles · Chemical damage · Rock slope · Stability

1 Introduction

Research on slope stability has always been a very important part in the field of geotechnical engineering construction. In the process of mining engineering, water conservancy and Hydropower Engineering and other construction projects, human beings inevitably need to reconstruct some surface rocks. At present, scholars at home and abroad have conducted in-depth research on the failure mechanism of conventional rock slopes and have achieved rich results. However, the related research on slope stability under the

multi-field coupling in cold regions is still insufficient. The reason is that many natural and human factors are involved; the destruction mode is more complicated and changeable and the theoretical knowledge involved is also more extensive [1–3]. In the initial stage of slope excavation, the stress field, seepage field and temperature field are redistributed to a new equilibrium state. However, with the change of the external ambient temperature and the influence of hydrochemical solutions, various physical fields are changing. The existing research results cannot explain the dynamic process well, so it is very important to study the stability of rock slope under the coupling of multiple physical fields [1, 3].

Multi-field coupling is a hot research issue, and domestic and foreign scholars have achieved some achievements in the research of multi-field coupling theory. The calculation methods for flexible systems used in slope stabilization were further studied by Blanco-Fernandez. An alternative modeling for flexible membranes anchored to the ground for soil slope stabilization was presented by using smoothed-particle hydrodynamics to model the unstable ground mass in a soil slope, employing a dynamic solve engine [4–6]. Based on the basic law of continuum mechanics, Exadak-tylos put forward the coupling model of freeze–thaw cycle

✉ Yi Luo
  yluo@whut.edu.cn

✉ Gang Wang
  gangw277842@whut.edu.cn

[1] School of Safety Science and Emergency Management, Wuhan University of Technology, Wuhan, China

[2] School of Civil Engineering and Architecture, Wuhan University of Technology, Wuhan, China

[3] Hubei Key Laboratory of Roadway Bridge and Structure Engineering, Wuhan University of Technology, Wuhan, China

with rock and soil as porous media material and applied the model to the freeze–thaw cycle test of porous media rock [7]. Tan et al. proposed a unified model of frost heave pressure in rocks in order to study the degradation mechanism of rock under low temperature conditions based on the theories of continuum mechanics, thermodynamics and segregation potential. The model attempted to unify the volume expansion theory, water immigration theory and combination theory [8–10]. Chen et al. derived a multiphase flow THM unity coupling mathematical model in porous media based on the principles of continuum mechanics and mixture theory. Based on the conservation of momentum, mass and energy of solid, liquid and gas three-phase systems, the coupling effects of stress–strain, water flow, gas transfer, steam transfer, heat transfer and porosity evolution were considered in the model. The results deepened the understanding of the control equation sets, constitutive relations and the calculation parameter characteristics of the multiphase flow THM unity coupling, thus laying a foundation for further study of the THMC unity coupling problem [11–14]. On the basis of heat transfer theory, seepage theory and frozen soil mechanics, Lai et al. deduced the mathematical mechanics model and control differential equation of temperature field, seepage field and stress field with phase transition. Then, he obtained the finite element calculation formula of this problem by means of Galerkin's method and applied it to the actual engineering construction [15, 16]. Many scholars have also studied the physical and mechanical properties of rock under the coupling action of hydrochemical solution and freeze–thaw. Deng et al. studied the changes of tensile strength and porosity of rock under the condition of hydrochemical solution and freeze–thaw cycle [17–19]. Li et al. carried out laboratory tests on the mechanical properties of rocks under the coupling action of acid solution and different hydrochemical solutions and freeze–thaw. He studied the degradation law of the mechanical properties such as the compressive strength and elastic modulus of rocks under the coupling action of hydrochemical solution and freeze–thaw and also analyzed the change law of the pore structure of rocks from the micro perspective [20–22].

In 2013, there was a serious landslide accident in Lhasa Jiama mining area of China. It resulted in serious casualties and property losses. The main cause of the accident was the deterioration of rock mechanical properties caused by freeze–thaw cycle and dynamic load [1]. As a kind of porous medium material, the water content in the pore structure of rock mass has a great influence on the damage degree caused by freeze–thaw cycle. Niu et al. deeply studied the geological conditions, environmental conditions, deformation laws and instability of the two slopes in the frozen soil region of the Qinghai–Tibet Plateau. It is found that the water content and displacement of the slope change obviously with the change of the external ambient temperature. Especially

after the shallow layer of the slope is frozen, the rise of groundwater level and the huge net water pressure inside the slope have a great impact on the stability of the slope, so it is necessary to pay attention to the drainage of the slope [23–26]. Li et al. conducted freeze–thaw cycles and uniaxial compression laboratory tests on rock samples and analyzed the freeze–thaw degradation mechanism of the rocks. He applied the laboratory tests to the stability analysis of an open-pit mine rock mass slope and calculated the change rule of safety coefficient before and after the freeze–thaw cycles of the slope by using Hoek–Brown criterion [3, 27, 28].

At present, scholars at home and abroad have carried out an in-depth study on the stability of conventional rock slope. However, the stress field, seepage field and chemical field of rock slopes under the action of freeze–thaw cycles are always in a dynamic change process. The research on the stability of rock slopes under the multi-field coupling is insufficient. It is of great significance for the prevention and control of slope stability in the process of engineering construction to study the dynamic changing process of slope in cold region under the multi-field coupling. The numerical simulation software COMSOL Multiphysics has a significant advantage in the research of multi-physical field coupling problem because of its fast computing power and the ability of multi-physical field direct coupling analysis. Based on it, the stability of rock slope under the action of multi-field coupling is studied in this paper.

2 Establishment and Verification of Numerical Model

2.1 Engineering Background

This paper takes the highway project from Jinghe to Yining County of G577 line in the mountain area on the north side of Tianshan Mountain as the project background (Fig. 1 is the geographical map of the project). Yining County has a continental climate with obvious characteristics of four seasons and large temperature difference between day and night. The annual average temperature is about 7.3 °C. The average temperature in January is −7.6 °C, the average temperature in July is 22.6 °C, the annual extreme minimum temperature is −34.3 °C, and the annual extreme maximum temperature is 39.7 °C. The terrain in this area is relatively special, so the rainfall is also rich, with a frost period of 202 days, and the area is also eroded by acid rain.

The annual average temperature in the project area is relatively low, but above 0 °C, the phreatic water and fissure water in the rock and soil layer are repeatedly frozen and melted. The temperature change of the original bottom layer is divided into two parts. The lower layer is the unfrozen
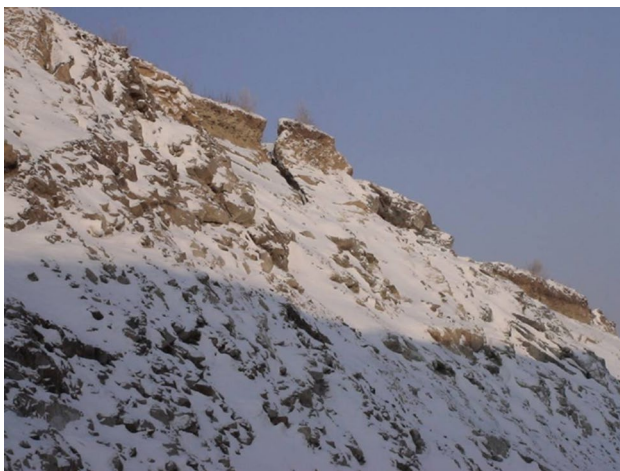
Fig. 1 Geographical map of the project

Fig. 2 Freeze–thaw slope in the project area

layer and the upper layer is the seasonal frozen layer (the freeze–thaw layer or the active layer) [29, 30]. For the slope formed by the excavation of the engineering construction, the changes of the surface temperature and the atmospheric temperature are basically the same due to human disturbance. Therefore, its surface is easy to be affected by

freeze–thaw cycle, resulting in slope stability reduction and risk of instability. It may cause geological disasters such as collapse, landslide and debris flow. Therefore, it is very meaningful to study the slope stability in the cold region (Fig. 2 shows the freeze–thaw slope map of the project area).

2.2 Establishment of Numerical Calculation Model

2.2.1 Establishment of Numerical Calculation Model

According to the report of "Engineering geological mapping and remote sensing interpretation of feasibility study of Jinghe to Yining highway project of G577 line" compiled by CCCC First Highway Survey and Design Institute, the representative rock slope is selected in this paper. According to the survey report, the lithology of the selected model slope is sandstone, with a length of 105 m and a height of 85 m, including a slope height of 45 m and a slope angle of 45°. Figure 3a is the dimension sketch of the slope geometric model and Fig. 3b is the meshing diagram of the slope geometric model. Due to the large temperature difference and abundant rainfall in the project area, considering the influence of acid rain on slope stability, the model also considers the influence of chemical field.

Fig. 3 Slope geometric model and meshing diagram

(a) Slope geometric model   (b) Slope meshing diagram
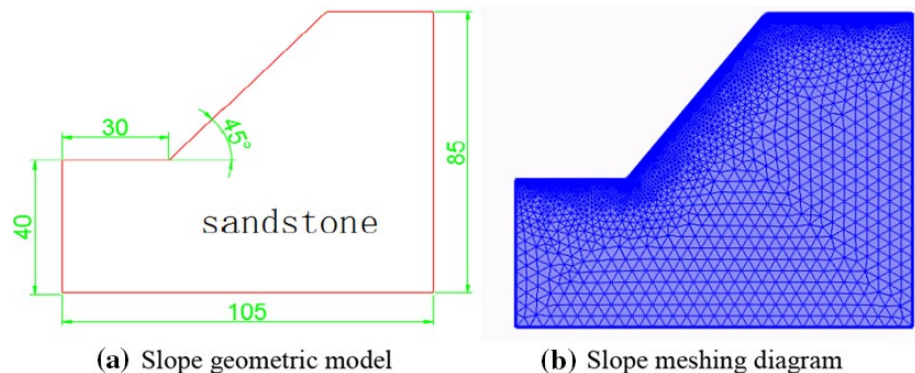
2.2.2 Determination of Numerical Calculation Parameters

According to the report of "Engineering geological mapping and remote sensing interpretation of feasibility study of Jinghe to Yining highway project of G577 line" and on-site sampling for laboratory tests, the numerical simulation calculation parameters are selected as shown in Table 1. The time step is one quarter (3 months), and the relative tolerance is 0.01. The mechanical response is subject to small displacements analysis. The material model used geotechnical materials and the Hoek–Brown strength criterion is selected in this paper.

2.2.3 Determination of Initial Value and Boundary Condition of Numerical Calculation

(a) Thermodynamic Conditions

The determination of the thermodynamic boundary conditions affects the change law of the slope temperature. According to reports and local meteorological data, the thawing starts slowly around March and April every year, and freeze starts around October. According to the historical temperature monitoring data of the climate department in the project area, the change law of the external temperature with time is simplified as Formula (1) [30, 31]. The change curve of the temperature with time in the project area is shown in Fig. 4.

$$T = 7.3 - 25.3\ \cos{(2\pi t/12)} \tag{1}$$

In the formula, T represents the ambient temperature with the unit of °C. t represents the time with the unit of d.

In this paper, convective heat transfer is the main heat exchange mode between the slope and the ambient environment. The boundary expression of convective heat transfer is shown in Formula (2). It is assumed that the initial state of the rock mass seasonal frozen layer is frozen state.

$$-\lambda \frac{\partial t}{\partial n} = h(t - t_f) \tag{2}$$

In the formula, h is the convective heat transfer coefficient and t_f is the ambient temperature.
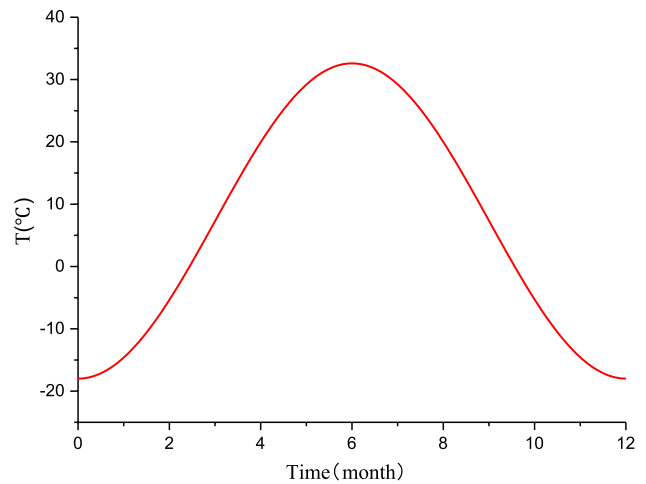

Fig. 4 The change curve of the temperature with time in the project area

Fig. 4 is the change curve of the temperature with time in the project area. The abscissa points in Fig. 4 represent the end of each month, where the 0–1 interval represents January.

(b) Mechanical Condition

The initial stress field is a very important part in the numerical simulation of geotechnical engineering. There are many factors that affect the initial stress field, including the depth of the research object, rock properties and the ambient environment. The main factor affecting the initial stress field is the dead weight stress field. For the solid mechanics module of the calculation model in this paper, the front and back, left and right, and bottom of the module are provided with roller support boundaries, and the upper is the free boundary.

(c) Seepage Condition

For the Darcy's Law module of the calculation model, the front and back, left and right, and bottom of the module are flow-free boundaries. The upper surface of the calculation model is free boundary, and the pressure is 0, that is, the initial pressure is 0 MPa. According to the boundary conditions and initial conditions, the static state of pore water under the action of gravity is defined. In fact, the seepage of pore water is caused by the change of temperature gradient.

Table 1 Initial thermodynamic and physical mechanical parameters of rock mass	Rock	E/GPa	Poisson ratio μ	Density ρ/km/m^3	Porosity	Compressive strength σ/MPa	Thermal conductivity W/(m °C)
	Sandstone	5.04	0.18	2740	0.045	35	2.7
	Water	–	–	1000	–	–	0.52
	Ice	–	–	916.8	–	–	2.21

(d) Hydrochemical Condition

Considering the influence of acid rain, groundwater and other hydrochemical factors on the slope, the calculation model also needs to add the transport of dilute species module. The frozen state and the melted state need to be analyzed separately. When the pore water is frozen, it is considered that no hydrochemical reaction occurs. When the pore water is in the melted state, the pore water will flow and the hydrochemical reaction will occur.

2.3 Verification of Numerical Calculation Model

Generally, the rain water is weakly acidic, and the pH value of rain water can be roughly considered as 5.6. Figure 5 shows the slope temperature distribution in January, April, July and early October of the year. Compared with the field measured temperature (0–2 m) close to the slope, it is found that the temperature distribution of numerical simulation is in good agreement with the measured data. The maximum frozen thickness of the model is 1.7 m, and it is consistent with the maximum frozen seasonal thickness of about 1.7 m in the report "Engineering geological mapping and remote

sensing interpretation of feasibility study of Jinghe to Yining highway project of G577 line." It shows that it is reliable for Formula (1) to represent the temperature change in the project area within 1 year and the calculation model.

Since the contact area with the ambient environment becomes larger and changes with the change of ambient temperature after the formation of slope excavation, the slope initial state of the numerical simulation is melting. This is related to the annual average temperature of the project area. It is set to 7.3 °C and calculated from the beginning of January of the year. It can be seen from Figs. 6, 7, 8 and 9 that the ambient temperature in January is relatively low and the average temperature is lower than 0 °C. The shallow layer of the slope is affected by the ambient temperature. The temperature gradually decreases and starts to freeze from the outside to the inside, with the maximum freezing thickness of 1.7 m. At this time, the pore water in the shallow layer of the slope stops flowing, and the hydrochemical reaction also temporarily stops. By about April, the ambient temperature will warm up, with an average temperature of about 10 °C. The frozen part of the shallow layer of the slope begins to melt, and the melting is gradually melting from the slope surface and the frozen maximum thickness at the same time.
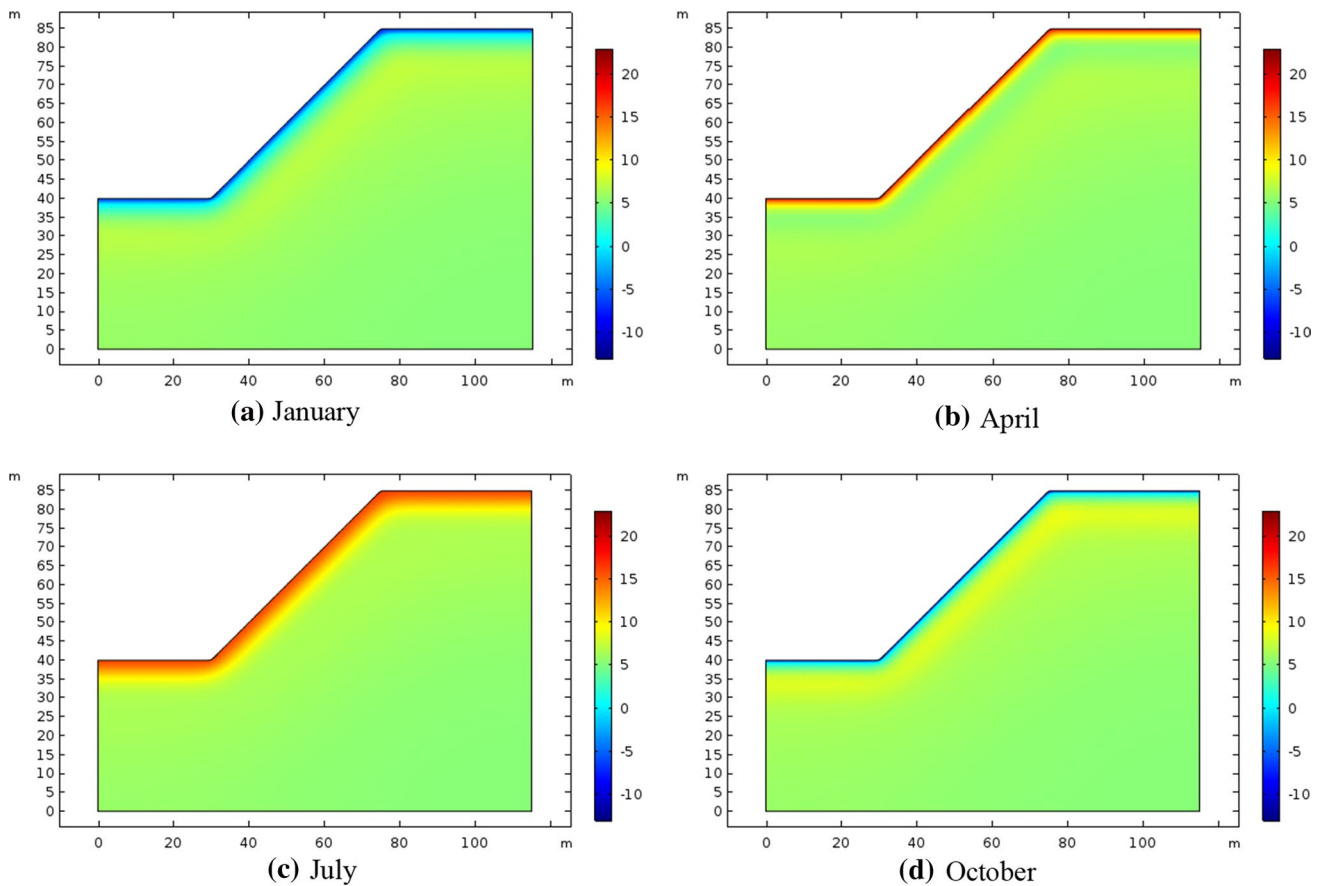

Fig. 5 Slope temperature distribution in different months

(a) 10 freeze-thaw cycles

(b) 20 freeze-thaw cycles

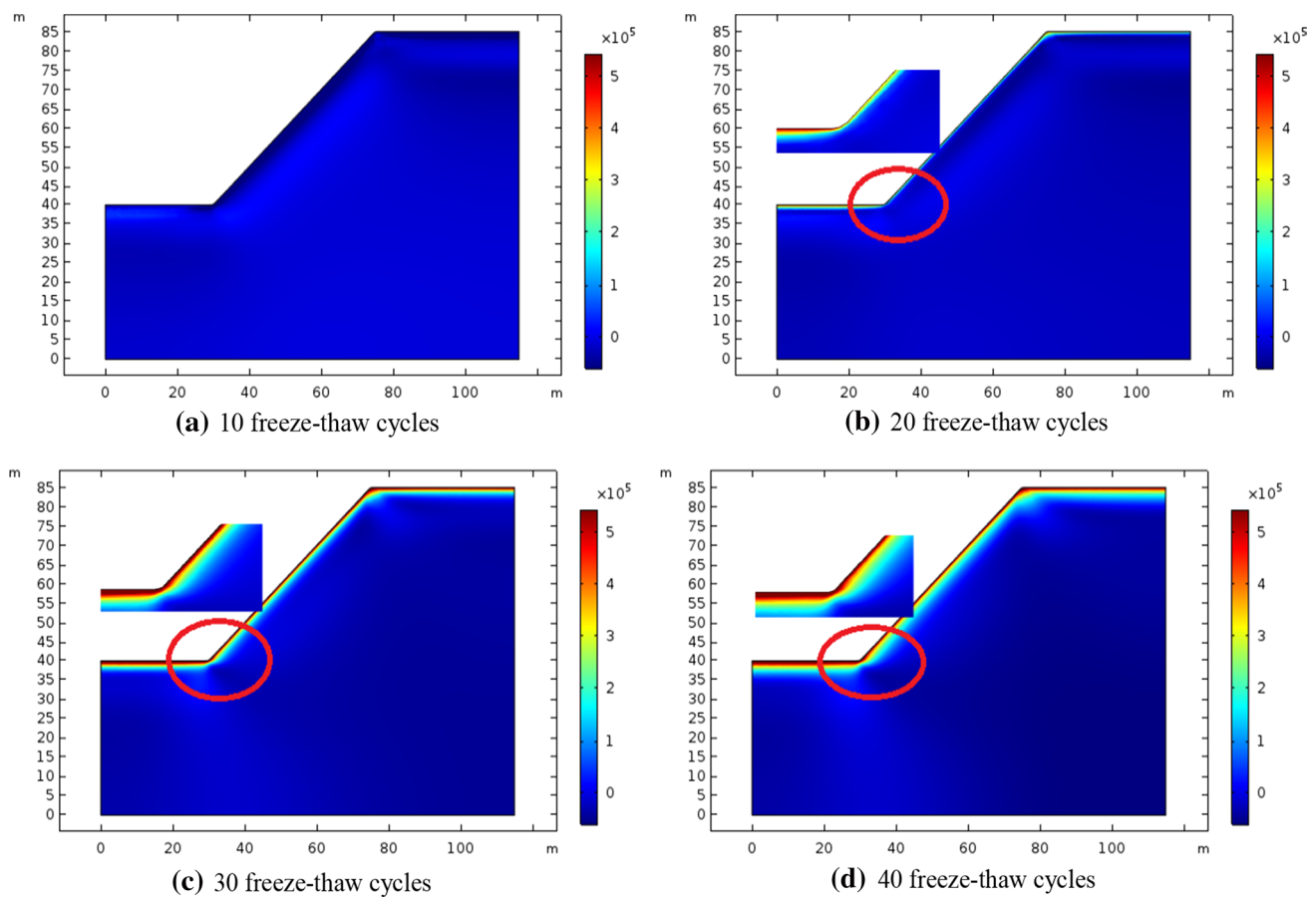**(c)** 30 freeze-thaw cycles

(d) 40 freeze-thaw cycles

Fig. 6 Change cloud chart of equivalent von Mises stress under different freeze–thaw cycles

Until July, the average temperature reaches 30 °C, the pore water in the entire slope is in a melting and flowing state, and the rate of hydrochemical reaction is the highest. Around October, the temperature begins to drop and the average temperature is below 0 °C. The surface of the slope begins to freeze gradually, and the hydrochemical reaction decreases with the decrease of temperature.

2.4 The Coupling Model of Stress Field, Seepage Field, Temperature Field and Chemical

(1) Stress Equilibrium Equation [32]

Stress equilibrium equation of frozen zone in rock mass. Because of the low temperature and the low content of unfrozen water in the frozen area of rock mass, it is assumed that there is no unfrozen water in the frozen area of rock mass, so the effective stress coefficient of unfrozen water is 0. Therefore, the stress balance equation of frozen zone in rock mass is:

$$\left\{ K_{ijkl} \left[\varepsilon_{kl} - \beta_r \left(T_r - T_{ro} \right) \delta_{kl} \right] + \alpha_i p_i \delta_{ij} \right\}_j + \rho_e \overrightarrow{X_i} = 0 \quad (3)$$

Stress equilibrium equation in the freezing zone of rock mass. The rock mass in this state is composed of rock matrix, unfrozen water and solid ice. Therefore, the stress balance equation of rock mass in the frozen area is:

$$\left\{ K_{ijkl} \left[\varepsilon_{kl} - \beta_r \left(T_r - T_{ro} \right) \delta_{kl} \right] + \left(\alpha_w p_w + \alpha_i p_i \right) \delta_{ij} \right\}_j + \rho_e \overrightarrow{X_i} = 0 \quad (4)$$

Stress equilibrium equation of unfrozen rock mass. The temperature of the unfrozen zone is above the freezing point. In this state, the water in the pores of the rock mass is all liquid and there is no ice. The effective stress coefficient of the ice in the rock mass is 0. Therefore, the stress balance equation of the unfrozen area of rock mass is as follows:

$$\left\{ K_{ijkl} \left[\varepsilon_{kl} - \beta_r \left(T_r - T_{ro} \right) \delta_{kl} \right] + \alpha_w p_w \delta_{ij} \right\}_j + \rho_e \overrightarrow{X_i} = 0 \quad (5)$$
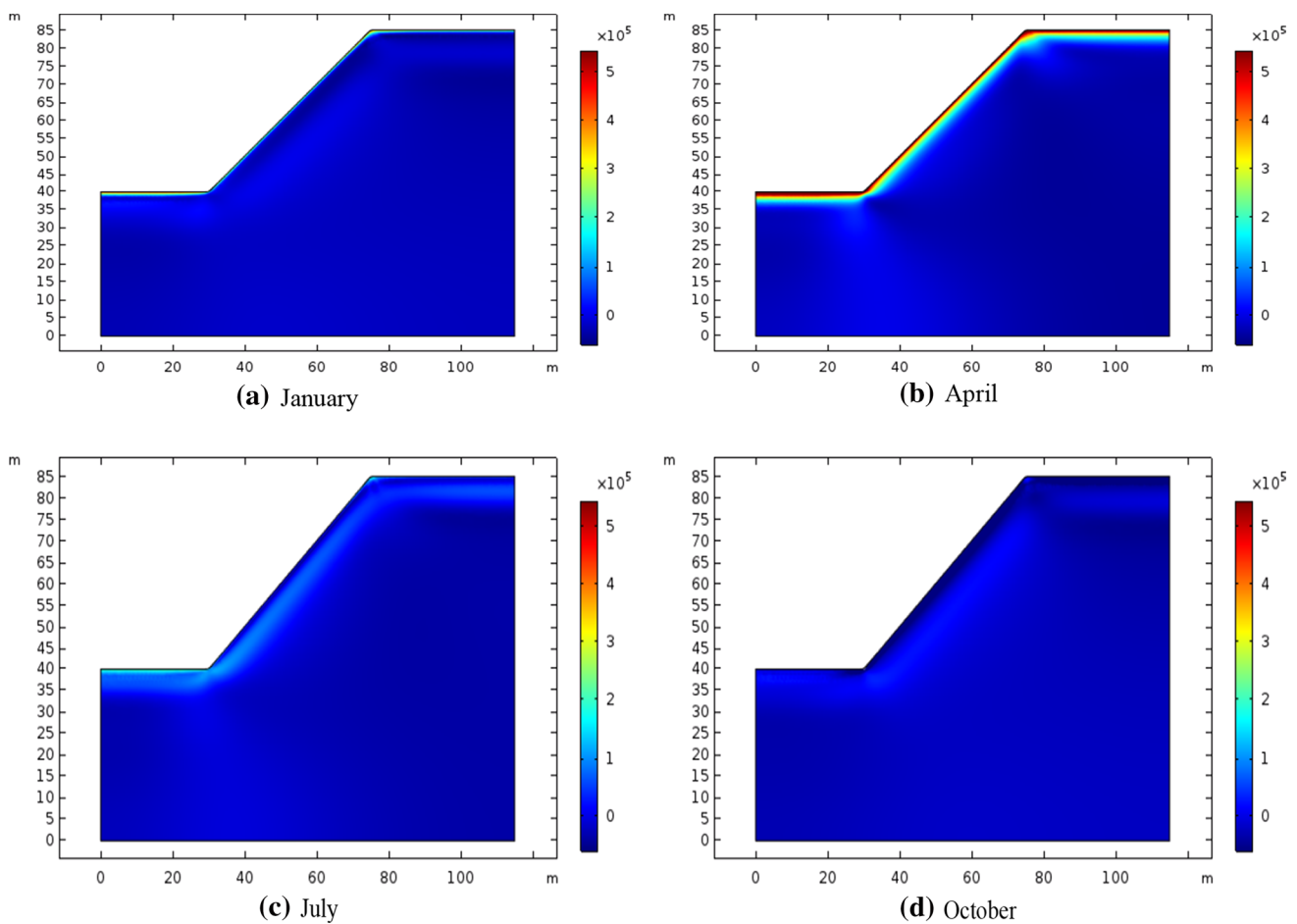
Fig. 7 Change cloud chart of equivalent von Mises stress in a freeze–thaw cycle (20 times of freeze–thaw cycles)

(2) Chemical transfer equation [33]. In the form of tensor, the chemical transfer equation can be obtained by introducing the hydrodynamic dispersion coefficient D.

$$\frac{\partial c_i}{\partial t} + \nabla \cdot \left(-D_i \nabla c_i \right) + u \cdot \nabla c_i = R_i \tag{6}$$

3 Analysis of Calculation Results

3.1 Slope Stress Change Under Multi-field Coupling

Figure 6 shows the change cloud chart of the equivalent von Mises stress of the slope with the number of freeze–thaw cycles in the freezing state under the action of multi-field coupling. Among them, Fig. 6a–d is change cloud charts of equivalent von Mises stress under 10, 20, 30 and 40 times of freeze–thaw cycles compared with 0 time of freeze–thaw cycle, respectively. The change cloud chart eliminates the effect of the stress redistribution caused by the initial stress

field and reflects the changing process of frost heave force with the number of freeze–thaw cycles in the process of the freeze–thaw cycle. It can be seen from the figure that the freeze–thaw cycle has a great impact on the frost heave force of the slope. With the increase of the number of freeze–thaw cycles, the frost heave force on the slope increases gradually. In the early stage of freeze–thaw cycle, the frost heave force is small. In the middle and late stages of freeze–thaw cycle, the increase rate of frost heave force is accelerated. The main reason is that under the coupling action of hydrochemical solution and freeze–thaw cycle, the pore structure of the shallow slope rock mass is developed and the porosity is increased. It provides more channels for the pore water to enter the rock mass. The frost heave force of the slope rock mass near the surface is obviously greater than that far away from the surface. With the increase of the depth of the slope, the frost heave force decreases. The equivalent stress of the slope rock mass beyond a certain depth is close to 0 and it indicates that the frost heave effect of the shallow slope rock mass is more obvious.
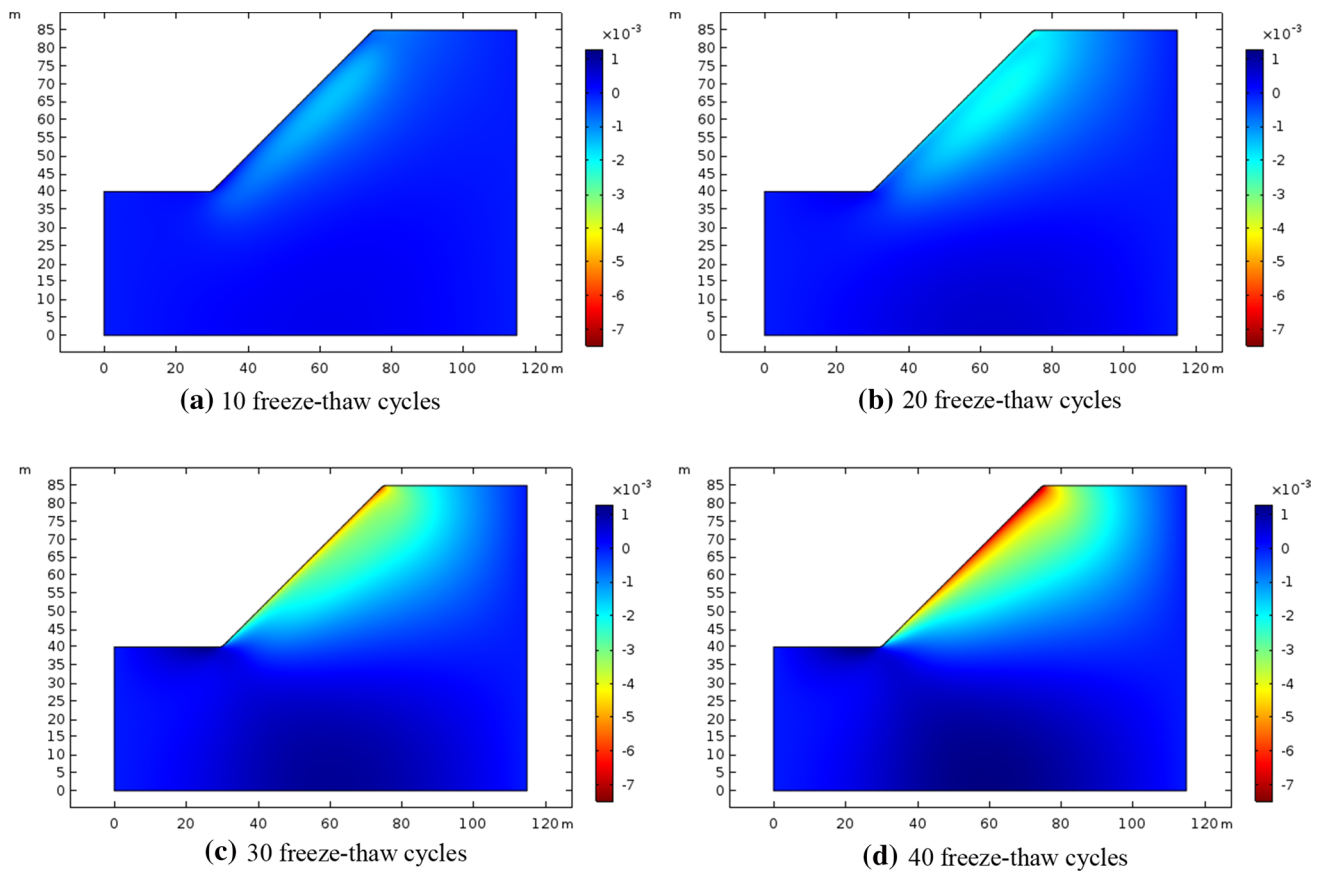
(a) 10 freeze-thaw cycles

(b) 20 freeze-thaw cycles

(c) 30 freeze-thaw cycles

(d) 40 freeze-thaw cycles

Fig. 8 Change cloud chart of displacements in the x direction of the slope under multi-field coupling

Fig. 9 Cloud chart of displacements in the y direction of the slope under multi-field coupling
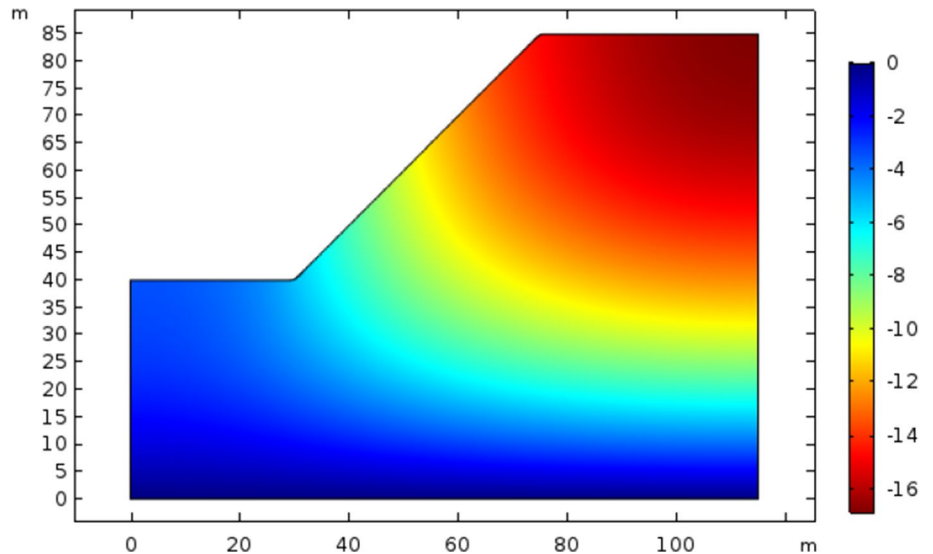

Figure 7 shows the frost heave force cloud chart of different months (early January, early April, early July and early October) in the 20th freeze–thaw cycle. Generally, the rock mass of the slope starts to melt around April and

freeze around October. From Fig. 6, it can be seen that the frost heave force of the slope in the frozen state is significantly greater than that of the slope in the melted state, and the frost heave force of the slope in the melted state is almost 0. With the periodic change of the atmospheric environment temperature, the frost heave force of the shallow layer of the slope also changes.

3.2 Change of Slope Displacement Under Multi-field Coupling

Figure 8 is a change cloud chart of the displacement of the slope in the x direction with the number of freeze–thaw cycles under multi-field coupling. Figure 9 is a cloud chart of displacements in the y direction under multi-field coupling. In this paper, there are many factors that affect the displacement of the slope, including frost heave in the process of freeze–thaw cycle, hydrochemical corrosion of hydrochemical solution and gravity field of the slope itself. Among them, the gravity field of the slope itself has the greatest impact on the overall displacement of the slope. In the process of freeze–thaw cycle, frost heave and hydrochemical corrosion of hydrochemical solution also have certain influence on the displacement of slope under the action of gravity field, mainly reflected in the shallow layer of slope. This is not obvious in the displacement cloud chart, especially the displacement in y direction, with small difference. Therefore, the displacement cloud chart in the y direction of slope rock mass under 40 times of freeze–thaw cycles and the displacement change cloud chart in the x direction of slope under different freeze–thaw cycles are given here.

Under the action of freeze–thaw cycle, the displacements of shallow layers of slope also present obvious periodic frost heave and thaw collapse with the freezing and thawing of shallow rock mass. If the average temperature of the ambient environment is lower, the maximum freezing thickness affected by the freeze–thaw cycle is greater and the frost heave displacement caused by freezing of the rock mass is greater. The direction of this frost heave displacement is upward. It can be seen from the displacement cloud chart of the slope in the x direction under the multi-field coupling that the displacements at the shallow slope toe and the slope top in the x direction are larger, while the displacements at the left and right positions in the middle of the slope are relatively small. But with the increase of the number of freeze–thaw cycles, the displacement of the slope top gradually increases and extends along the slope to the middle and lower parts of the slope. It can be seen from the displacement cloud chart in the y direction under the multi-field coupling that the displacement at the slope top in the y direction is the largest and the displacement at the bottom of the slope in the y direction is the smallest.

3.3 Changes of Slope Damage Under Multi-field Coupling

The equivalent plastic strain is used to define the damage variable and the damage analysis of slope under multi-field coupling is carried out. Figure 10 shows the damage cloud chart of the slope in the frozen state under different freeze–thaw cycles.

Figure 10 is a change cloud chart of the damage degree with the number of freeze–thaw cycles when the slope is in the frozen state under multi-field coupling. Figure 10a–d is damage change cloud charts after 10, 20, 30 and 40 times of freeze–thaw cycles, respectively. It can be seen from the figures that with the increase of freeze–thaw cycles, the damage degree of the slope increases obviously under multi-field coupling. After 10 times of freeze–thaw cycles, the damage degree of slope is not obvious. After 20 times of freeze–thaw cycles, obvious damage areas can be seen on the slope, which are mainly reflected in the slope toe and the shallow area parallel to the slope. When the slope undergoes 30 times and 40 times of freeze–thaw cycles, the damage areas gradually expand. The damage area at the slope toe is centered at the slope toe and gradually develops deeper into the slope. On the slope surface, the damage area develops deeper into the slope parallel to the slope surface, but the area with larger damage does not exceed the maximum freezing depth. This is because the freeze–thaw cycle only occurs above the maximum freezing depth. Under the repeated frost heaving, the damage of the slope rock mass in this range gradually accumulates, while the rock mass outside this range will not be affected by the freeze–thaw cycle. The rock mass is always in a melting state and the content of groundwater is low. The structure of rock mass is relatively complete and the flow of groundwater in the slope rock mass is also very slow. Therefore, the damage degree is very small. Compared with the damage degree of slope toe and shallow layer, it can be ignored. The damage evolution process of slope rock mass is consistent with the change law of its stress and displacement.

The damage of the slope is gradually accumulated under multi-field coupling, and the influencing factors are also various, mainly reflected in the frost heave damage caused by the freeze–thaw cycle, the hydrochemical corrosion damage caused by the acid water solution, and the damage caused by the stress field of the slope itself. The effects of these factors are very slow and can only be manifested under long-term cumulative effects.
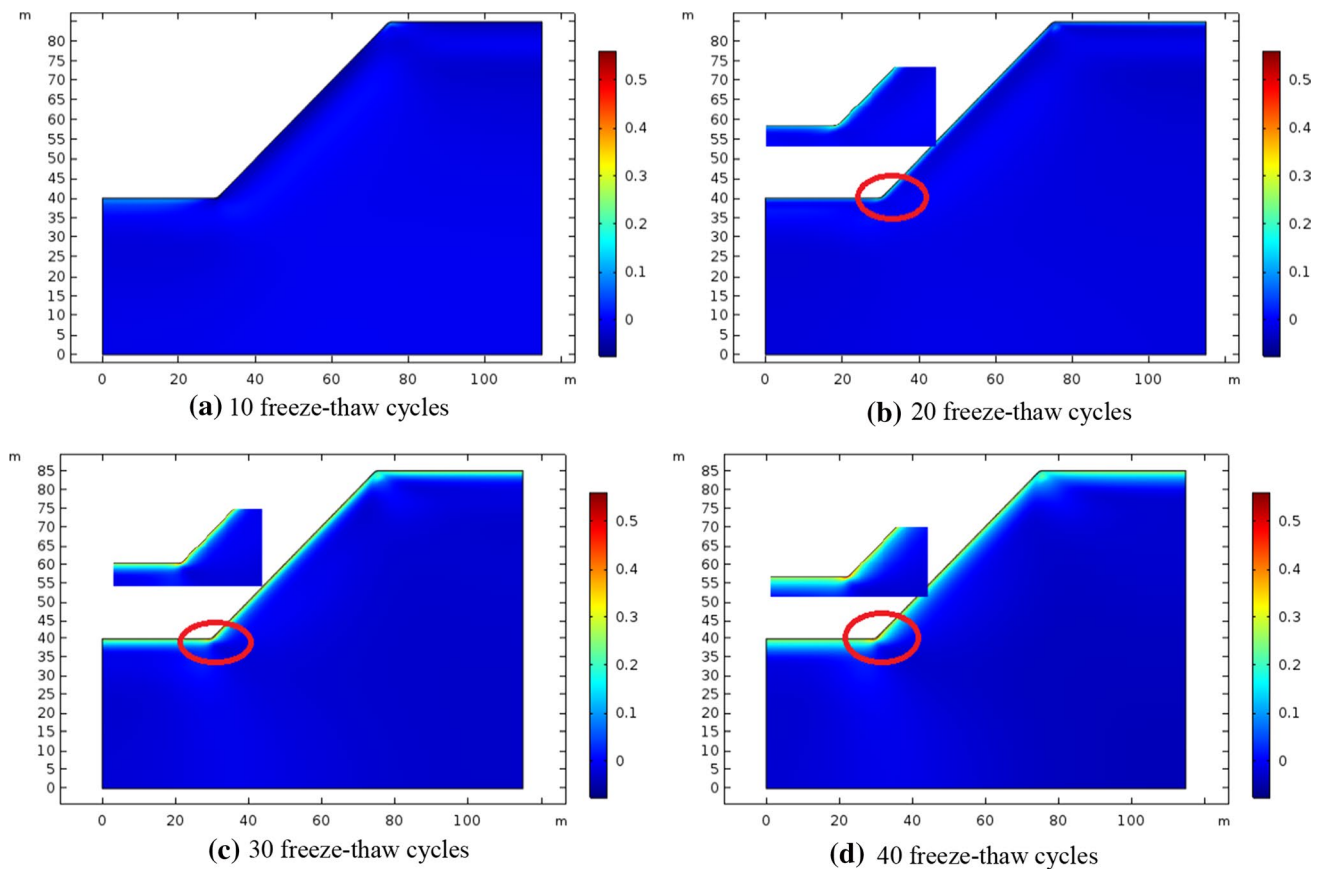
(a) 10 freeze-thaw cycles

(b) 20 freeze-thaw cycles

(c) 30 freeze-thaw cycles

(d) 40 freeze-thaw cycles

Fig. 10 Change cloud chart of slope damage under multi-field coupling

4 Stability Analysis of Rock Slope Under Multi-field Coupling

The time effect characteristic of rock slope stability in the alpine region is very obvious. It is a dynamic equilibrium problem. The number of freeze–thaw cycles has a positive correlation with slope stability. With the increase of the number of freeze–thaw cycles, the possibility of potential landslide in the engineering area is greater. Under the action of freeze–thaw cycle, the rock mass in the seasonal frozen layer has the effect of frost heave and thaw shrinkage. The porosity of rock mass increases gradually, its mechanical parameters deteriorate gradually, and its potential sliding surface is parallel to the slope surface. By using yield approach index (YAI) to study the stability of rock slope under multi-field coupling, it can well reflect the change rule of local damage degree of the shallow layer of the slope with time. Based on the theory of YAI, the slope stability is analyzed from the freezing, thawing and freeze–thaw process states of the shallow layer of the slope.

4.1 Stability Analysis of Rock Slope with Thawed Seasonal Frozen Layer

In July of each year, the average temperature of the project area is the highest, reaching about 30 °C. The pore water of the whole slope is in a state of melting and flowing, with the fastest flow rate and the largest hydrochemical reaction rate. The stability of rock slope is studied in July every year when the seasonal frozen layer is thawed.

YAI is used to express the damage degree at a certain point of the study object. For the local stability analysis of slope under the multi-field coupling, it can select the area with greater impact on the seasonal frozen layer slope for analysis. Generally, $YAI \leq 0.6$ is the selection standard. The local YAI can be expressed as:

$$YAI_{local} = \frac{\sum\limits_{i=0}^{n} Y_i V_i}{\sum\limits_{i=0}^{n} V_i} \tag{7}$$

In the formula Y_i—YAI of each study unit; V_i—the volume of the YAI corresponding to the study unit.
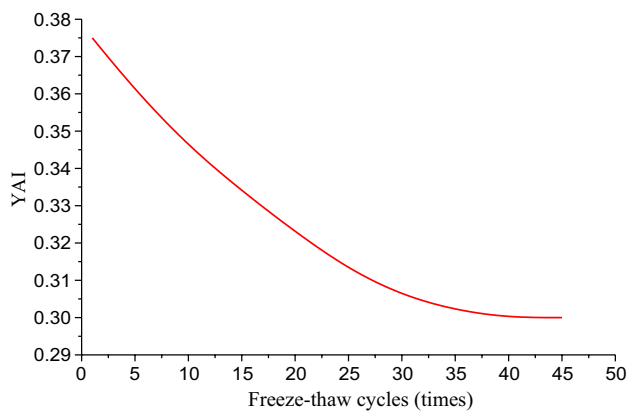
Fig. 11 Change curve of local YAI with the number of freeze–thaw cycles in thawed state of slope

The smaller the value of YAI is, the greater the damage degree is. Gao Liyan, Li Guofeng, etc. [34, 35] pointed out that when $YAI \geq 0.2$, this point is in a temporary safe state. $0.2 < YAI \leq 0.6$ indicates a damaged area, $0 < YAI \leq 0.2$ indicates an area close to damage, and $YAI = 0$ indicates that it has been damaged.

Figure 11 shows the change curve of local YAI with the number of freeze–thaw cycles in thawed state of slope. It can be seen from the figure that with the increase of the number of freeze–thaw cycles, the YAI of the slope gradually decreases. When the number of freeze–thaw cycles reaches 40, the YAI of the slope reaches 0.3 and remains stable. Although the local YAI is more than 0.2, the YAI of some study units has been less than 0.2 or even equals to 0. It indicates that after 40 times of freeze–thaw cycles, some parts of the slope have been in a state of damage or critical damage and the slope may be unstable.
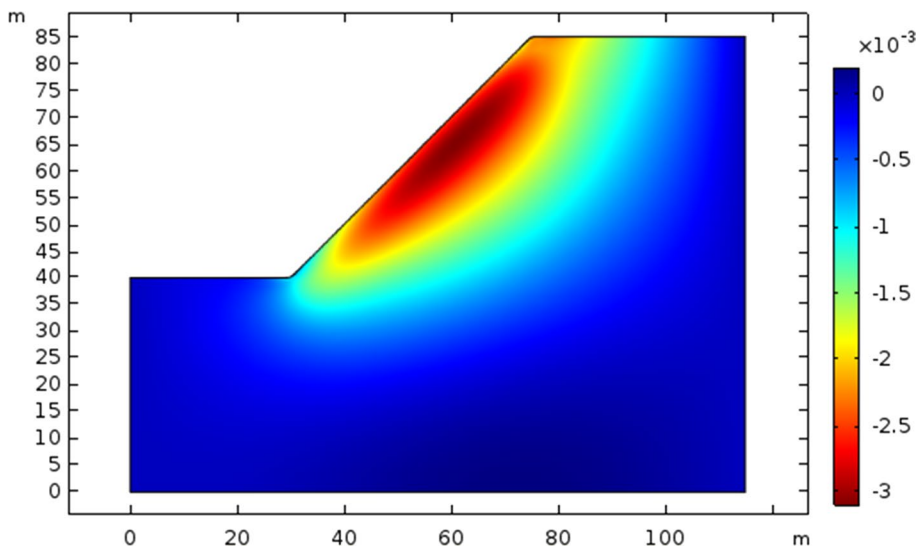
Figure 12 shows the cloud chart of slope displacement in x direction under 40 times of freeze–thaw cycles. It can be seen from the figure that when the YAI of the slope reaches 0.3, the maximum displacement in x direction of the slope surface closer to the slope toe reaches 7.6 mm, with a larger displacement increment. Figure 13 shows the cloud chart of slope damage under 40 times of freeze–thaw cycles. It can be seen from the figure that when the YAI of the slope reaches 0.3, the damage degree of the slope at the position where the slope surface is closer to the foot of the slope is the largest. The results of displacement change and damage change of slope are consistent with those of local YAI curves. Therefore, when the number of freeze–thaw cycles reaches 40, the slope is likely to lose stability and protective measures need to be taken.

4.2 Stability Analysis of Rock Slope with Frozen Seasonal Frozen Layer

In January of each year, the average temperature in the project area is the lowest, reaching about—7.6 °C. The pore water in the shallow layer of the whole slope is frozen and the hydrochemical reaction has stopped. When the seasonal frozen layer of rock slope is frozen, the stability of the slope is studied according to the research standard of January every year. Figure 14 shows the change curve of local YAI with the number of freeze–thaw cycles in frozen state of slope. It can be seen from the figure that with the increase of the number of freeze–thaw cycles, the YAI of the slope decreases gradually. When the number of freeze–thaw cycles reaches 40, the YAI of the slope reaches 0.376. Compared with Fig. 11, it can be found that the YAI of the frozen slope is significantly greater than that of the thawed slope, indicating that the frozen slope is more stable and less prone to instability.

Fig. 12 Cloud chart of slope displacement in X direction in the thawed state under 40 times of freeze–thaw cycles

Fig. 13 Cloud chart of slope damage in the thawed state under 40 times of freeze–thaw cycles
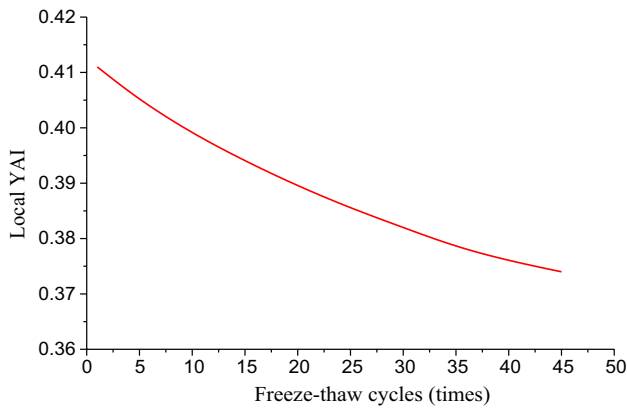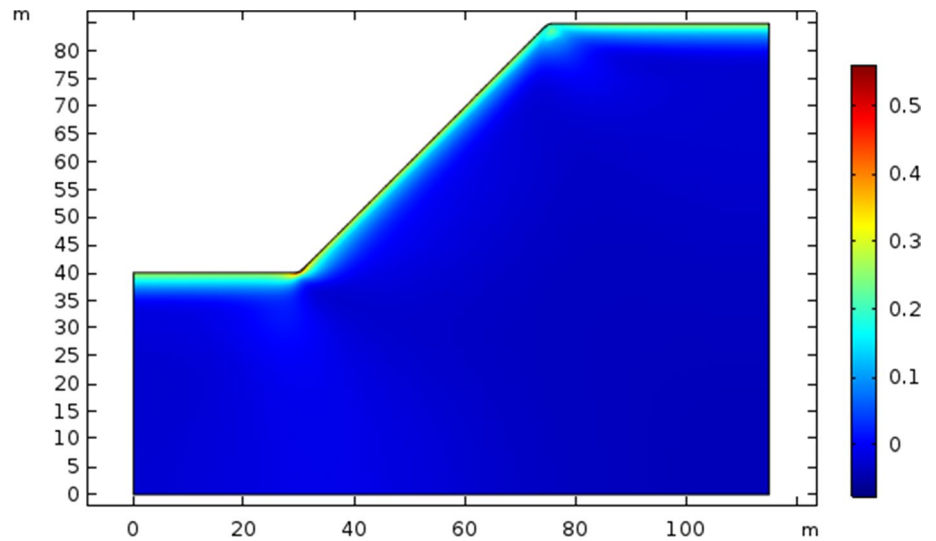

Fig. 14 Change curve of local YAI with the number of freeze–thaw cycles in frozen state of slope

Figure 15 shows the cloud chart of slope displacement in X direction in the frozen state under 40 times of freeze–thaw cycles. It can be seen from the figure that the maximum displacement in X direction of the slope surface closer to the slope toe reaches 9.7 mm, with a larger displacement increment. This is larger than the X direction displacement increment at the same position in the thawed state. It is caused by the frost heave effect in the frozen state. Figure 16 shows the cloud chart of slope damage in the frozen state under 40 times of freeze–thaw cycles. It can be seen from the figure that the damage degree of the slope surface closer to the slope toe and the shallow layer of the slope is the largest, but the possibility of instability is small due to its frozen state. Therefore, when the number of freeze–thaw cycles reaches

Fig. 15 Cloud chart of slope displacement in X direction in the frozen state under 40 times of freeze–thaw cycles
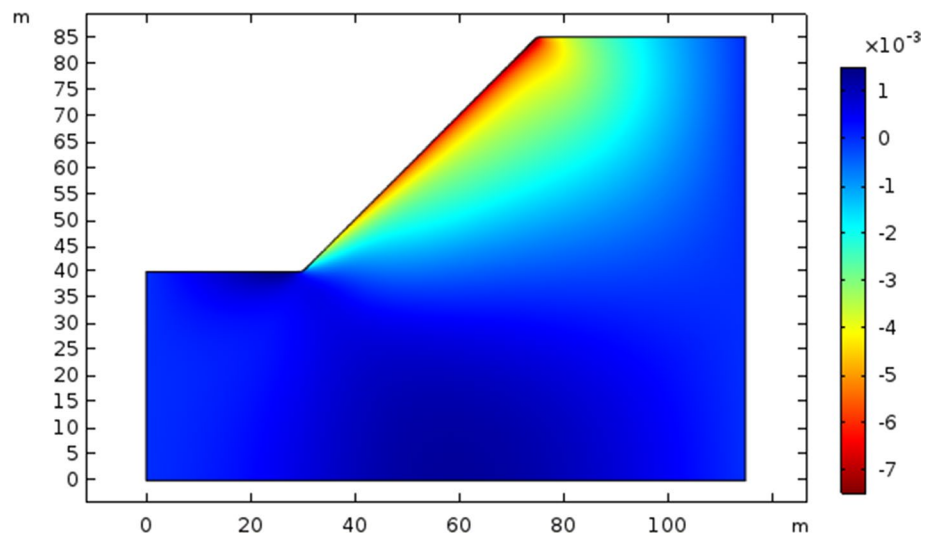
Fig. 16 Cloud chart of slope damage in the frozen state under 40 times of freeze–thaw cycle
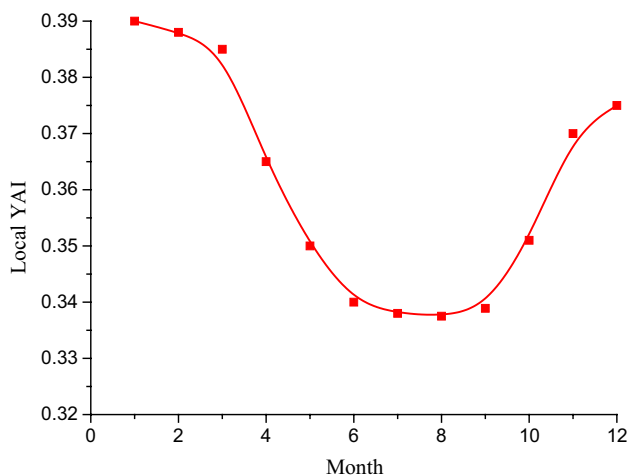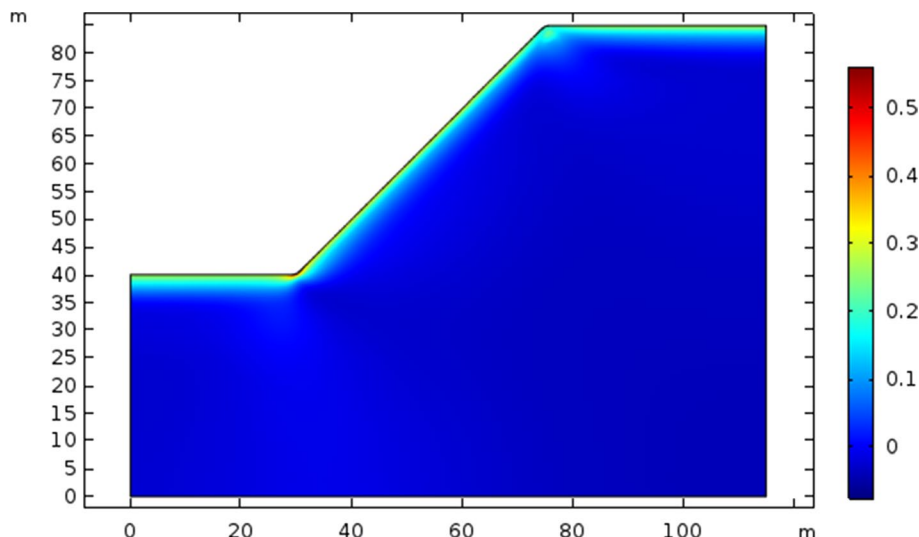
Fig. 17 Change curve of local YAI in a freeze–thaw cycle

40, the stability of the slope in the frozen state is stronger than that in the thawed state.

4.3 Effect of Freeze–Thaw Cycle on Slope Stability Under Multi-field Coupling

Taking the 20th freeze–thaw cycle as the research object, the stability of rock slope in a freeze–thaw cycle is analyzed. Figure 17 shows the change curve of local YAI of slope rock mass with months in a freeze–thaw cycle. It can be seen from the figure that the stability of the freeze–thaw slope has a very significant timeliness. With the increase of the freezing depth, the stability of the slope is enhanced, and with the increase of the melting depth, the stability of the slope is gradually weakened. Therefore, it is necessary to select appropriate research standards for slope stability analysis under multi-field coupling. In this paper, the worst

time of slope stability in a year (i.e., July) is selected as the research standard to analyze the stability of the engineering slope. It is consistent with the conclusion of the engineering geological report.

5 Conclusion

In this paper, COMSOL Multiphysics numerical simulation software and numerical simulation methods are adopted. Based on the coupling theory of rock stress field, seepage field, temperature field, and chemical field, and field test data, the stability of rock slope under the of multi-field coupling is studied under the research background of the highway slope of Jinghe to Yining County of G577 line. Combining local meteorological data such as temperature change range, rainfall range, pH value of acid rain and geological investigation reports, the stability of rock slope under the multi-field coupling is studied. The change law of the relevant parameters such as the stress, temperature, deformation and damage of the highway slope in the engineering area is studied, and the stability of the highway slope in the engineering area is analyzed. It provides a certain theoretical basis for the engineering construction in the cold area. With the increasing complexity of cold region engineering, the research on the cold region engineering problem under the action of multi-field coupling will be paid more attention. The conclusion is as follows:

(1) According to the geological investigation report and meteorological data, the temperature variation equation of the project area with time is obtained. Based on the study of multi-field coupling theory, the appropriate numerical calculation parameters, initial values

and boundary conditions (including thermodynamic conditions, seepage conditions and hydrochemical conditions) are selected to establish the numerical calculation model, and the rationality of the numerical calculation model is verified.

(2) According to the established numerical calculation model, the maximum frozen thickness of the slope is 1.7 m. The change law of stress, displacement and damage of the slope in the engineering area under the multi-field coupling is studied. With the increase of the number of freeze–thaw cycles, the stress field and displacement field of the shallow layer of the slope change accordingly, and the damage gradually accumulates.

(3) Based on the evaluation method of the YAI of slope stability, the slope stability analysis is carried out. The stability of the slope is analyzed from the freezing, thawing and freeze–thaw process states of the shallow layer of the slope.

Data Availability Some or all data, models, or code that support the findings of this study are available from the corresponding author upon reasonable request.

References

1. Ke, B.; Zhou, K.P.; Xu, C.S.; Deng, H.W.; Li, J.L.; Bin, F.: Dynamic mechanical property deterioration model of sandstone caused by freeze–thaw weathering. Rock Mech. Rock Eng. **51**(9), 2791–2804 (2018)

2. Zhang, C.; Pu, C.; Cao, R.; Jiang, T.; Huang, G.: The stability and roof-support optimization of roadways passing through unfavorable geological bodies using advanced detection and monitoring methods, among others, in the Sanmenxia Bauxite Mine in China's Henan Province. Bull. Eng. Geol. Environ. **78**(7), 5087–5099 (2019)

3. Li, J.; Zhou, K.; Liu, W.; Zhang, Y.: Analysis of the effect of freeze–thaw cycles on the degradation of mechanical parameters and slope stability. Bull. Eng. Geol. Environ. **77**(2), 573–580 (2018)

4. Blanco-Fernandez, E.; Castro-Fresno, D.; Diaz, J.J.D.; Lopez-Quijada, L.: Flexible systems anchored to the ground for slope stabilisation: critical review of existing design methods. Eng. Geol. **122**(3–4), 129–145 (2011)

5. Blanco-Fernandez, E.; Castro-Fresno, D.; Diaz, J.J.D.; Diaz, J.: Field measurements of anchored flexible systems for slope stabilisation: evidence of passive behaviour. Eng. Geol. **153**, 95–104 (2013)

6. Blanco-Fernandez, E.; Castro-Fresno, D.; Diaz, J.J.D.; Navarro-Manso, A.; Alonso-Martinez, M.: Flexible membranes anchored to the ground for slope stabilisation: numerical modelling of soil slopes using SPH. Comput. Geotechn. **78**, 1–10 (2016)

7. Exadaktylos, G.: Freezing–thawing model for soils and rocks. J. Mater. Civ. Eng. **18**(2), 241–249 (2006)

8. Tan, X.; Chen, W.; Liu, H.; Wang, L.; Ma, W.; Chan, A.H.C.: A unified model for frost heave pressure in the rock with a penny-shaped fracture during freezing. Cold Reg. Sci. Technol. **153**, 1–9 (2018)

9. Tan, X.; Chen, W.; Tian, H.; Cao, J.: Water flow and heat transport including ice/water phase change in porous media: numerical simulation and application. Cold Reg. Sci. Technol. **68**(1–2), 74–84 (2011)

10. Tan, X.; Chen, W.; Yang, J.; Cao, J.: Laboratory investigations on the mechanical properties degradation of granite under freeze–thaw cycles. Cold Reg. Sci. Technol. **68**(3), 130–138 (2011)

11. Chen, Y.; Zhou, C.; Jing, L.: Modeling coupled THM processes of geological porous media with multiphase flow: theory and validation against laboratory and field scale experiments. Comput. Geotech. **36**(8), 1308–1329 (2009)

12. Chen, Y.; Li, D.; Jiang, Q.; Zhou, C.: Micromechanical analysis of anisotropic damage and its influence on effective thermal conductivity in brittle rocks. Int. J. Rock Mech. Min. Sci. **50**(1), 102–116 (2012)

13. Chen, Y.; Zhou, C.; Sheng, Y.: Formulation of strain-dependent hydraulic conductivity for a fractured rock mass. Int. J. Rock Mech. Min. Sci. **44**(7), 981–996 (2007)

14. Nishimura, S.; Gens, A.; Olivella, S.; Jardine, R.: THM-coupled finite element analysis of frozen soil: formulation and application. Géotechnique **59**(3), 159 (2009)

15. Yuanming, L.; Ziwang, W.; Songyu, L.; Xuejun, D.: Nonlinear analyses for the semicoupled problem of temperature, seepage, and stress fields in cold region retaining walls. J. Therm. Stress. **24**(12), 1199–1216 (2001)

16. Lai, Y.; Zhang, S.; Zhang, L.; Xiao, J.: Adjusting temperature distribution under the south and north slopes of embankment in permafrost regions by the ripped-rock revetment. Cold Reg. Sci. Technol. **39**(1), 67–79 (2004)

17. Deng, H.W.; Dong, C.F.; Li, J.L.; Zhou, K.P.; Tian, W.G.; Zhang, J.: Experimental study on sandstone freezing–thawing damage properties under condition of water chemistry. Appl. Mech. Mater. **608–609**, 726–731 (2014)

18. Yu, J.; Chen, X.; Li, H.; Zhou, J.W.; Cai, Y.Y.: Effect of freeze–thaw cycles on mechanical properties and permeability of red sandstone under triaxial compression. J. Mt. Sci. **12**(1), 218–231 (2015)

19. Deng, H.W.; Yu, S.T.; Deng, J.R.: Damage characteristics of sandstone subjected to coupled effect of freezing–thawing cycles and acid environment. Adv. Civ. Eng., Art. no. 3560780 (2018)

20. Li, X.P.; Qu, D.X.; Luo, Y.; Ma, R.Q.; Xu, K.; Wang, G.: Damage evolution model of sandstone under coupled chemical solution and freeze–thaw process. Cold Reg. Sci. Technol. **162**, 88–95 (2019)

21. Qu, D.X.; Li, D.K.; Li, X.P.; Yi, L.; Xu, K.: Damage evolution mechanism and constitutive model of freeze–thaw yellow sandstone in acidic environment. Cold Reg. Sci. Technol. **155**, 174–183 (2018)

22. Cai, Y.Y.; Yu, J.; Fu, G.F.; Li, H.: Experimental investigation on the relevance of mechanical properties and porosity of sandstone after hydrochemical erosion. J. Mt. Sci. **13**(11), 2053–2068 (2016)

23. Niu, F.-J.; Cheng, G.-D.; Lai, Y.-M.; Jin, D.-W.: Instability study on thaw slumping in permafrost regions of Qinghai–Tibet Plateau. Chin. J. Geotech. Eng. Chin. Ed. **26**, 402–406 (2004)

24. Wang, Q.; et al.: Observational study on the active layer freeze–thaw cycle in the upper reaches of the Heihe River of the northeastern Qinghai–Tibet Plateau. Quat. Int. **440**, 13–22 (2017)

25. Niu, F.; Cheng, G.; Ni, W.; Jin, D.: Engineering-related slope failure in permafrost regions of the Qinghai–Tibet Plateau. Cold Reg. Sci. Technol. **42**(3), 215–225 (2005)

26. Wei, M.; Fujun, N.; Satoshi, A.; Dewu, J.: Slope instability phenomena in permafrost regions of Qinghai–Tibet Plateau, China. Landslides **3**(3), 260–264 (2006)

27. Kolay, E.: Modeling the effect of freezing and thawing for sedimentary rocks. Environ. Earth Sci. **75**(3), 210 (2016)

28. Ince, I.; Fener, M.: A prediction model for uniaxial compressive strength of deteriorated pyroclastic rocks due to freeze–thaw cycle. J. Afr. Earth Sci. **120**, 134–140 (2016)

29. Dobiński, W.: The cryosphere and glacial permafrost as its integral component. Cent. Eur. J. Geosci. **4**(4), 623–640 (2012)

30. Shuanhai, X.U.; et al.: Damage test and degradation model of saturated sandstone due to cyclic freezing and thawing of rock slopes of open-pit coal mine. Chin. J. Rock Mech. Eng. **35**, 2561–2571 (2016)

31. Liu, N.; Li, N.; Wang, L.; Xu, S.: Coupled analysis of thermo-hydro-mechanical field for Huashixia roadbed. Phys. Numer. Simul. Geotech. Eng. **14**, 70 (2014)

32. Wegmann, M.; Gudmundsson, G.H.; Haeberli, W.: Permafrost changes in rock walls and the retreat of alpine glaciers: a thermal modelling approach. Permafr. Periglac. Process. **9**(1), 23–33 (1998)

33. Su, B.; Zhang, W.; Sheng, J.; Xu, X.; Zhan, M.; Liu, J.: Study of permeability in single fracture under effects of coupled fluid flow and chemical dissolution. Rock Soil Mech. **31**(11), 3361–3366 (2010)

34. Gao, L.; Yu, G.; Zhao, J.; Wan, X.; Yuan, C.: Analysis and application of yielding approach based on material strength criteria. J. Chongqing Univ. **5**, 10 (2016)

35. Guofeng, L.I.; Ning, L.I.; Liu, N.; Zhu, C.: Practical algorithm of THM coupling process with ice-water phase change based on FLAC ~ (3D). Chin. J. Rock Mech. Eng. **36**, 3841–3851 (2017)